Article

Direct Observation of Atoms Entering and Exiting l-Alanyl-l-valine Nanotubes by Hyperpolarized Xenon-129 NMR

Chi-Yuan Cheng, and Clifford R. Bowers

J. Am. Chem. Soc., **2007**, 129 (45), 13997-14002• DOI: 10.1021/ja074563n • Publication Date (Web): 18 October 2007

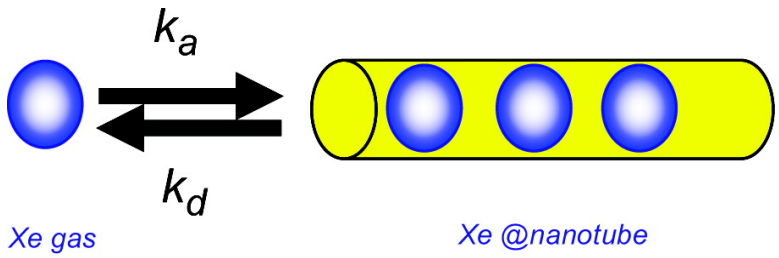

More About This Article

Additional resources and features associated with this article are available within the HTML version:

- Supporting Information
- Links to the 5 articles that cite this article, as of the time of this article download
- Access to high resolution figures
- Links to articles and content related to this article
- Copyright permission to reproduce figures and/or text from this article

View the Full Text HTML

J|A|C|S
ARTICLES
Published on Web 10/18/2007

Direct Observation of Atoms Entering and Exiting L-Alanyl-L-valine Nanotubes by Hyperpolarized Xenon-129 NMR

Chi-Yuan Cheng and Clifford R. Bowers*

Contribution from the Chemistry Department, University of Florida, P.O. Box 117200, Gainesville, Florida 32611

Received July 6, 2007; E-mail: russ@ufl.edu

Abstract: The kinetics of gas → channel and channel → gas exchange of Xe in self-assembled L-alanyl-L-valine (AV) nanotubes was facilitated by continuous flow hyperpolarized xenon-129 two-dimensional exchange NMR spectroscopy. Cross-peaks due to gas atoms entering or exiting were observed at Xe pressures of 92, 1320, and 3300 mbar, corresponding to Xe fractional occupancies ranging from 0.047 to 0.64. At each pressure, the rate of desorption from the channels was determined by fitting the mixing time dependence of the cross-peak and diagonal-peak signals to a magnetization exchange model, assuming steady-state Langmuir adsorption under hyperpolarized gas flow conditions. The observed rate constant for desorption of Xe from AV nanotubes decreased from 4.5 s^{-1} to 2.0 s^{-1} over the occupancy range studied, a finding that is consistent with a decrease in the diffusivity in the channels.

Introduction

Recent interest in the adsorption, exchange, and transport properties of nanotube materials has been stimulated by important potential applications, such as gas separation[1−11] and nanofluidics.[12−15] Theoretical studies predict that confinement within one-dimensional channels can radically alter molecular dynamics and transport properties.[14−18] For instance, when the channels are occupied by particles too large to pass one another, single-file diffusion (SFD) may occur at certain time scales.[17−22] Although such phenomena have been confirmed in macroscopic model systems,[23−25] only a few experimental studies of molecular SFD[19−21] have been reported to date. Channel boundary and desorption barrier effects, particle−particle/particle−wall interactions, and crossover between different diffusion time-scaling regimes can be numerically simulated for idealized nanotube systems. However, experimental validation has been hampered by the lack of suitable techniques for investigating the details of molecular exchange and diffusion in real nanotube materials. While adsorption properties have been characterized, molecular exchange and diffusion localized near single-file channel openings has never been investigated experimentally. Such will be the topic of this study of Xe exchange in polycrystalline L-alanyl-L-valine (AV) nanotubes.

The channels of AV, which are lined with $-CH_3$ groups, have an inner diameter of 5.13 Å.[26−29] Xenon, with a van der Waals diameter of 4.5 Å, has a high propensity for adsorption into the hydrophobic channels of AV.[27,29] Xenon-129 is particularly well-suited for the NMR characterization of nanoporosity.[27−40] Its

(1) Ackerman, D. M.; Skoulidas, A. I.; Sholl, D. S.; Johnson, J. K. *Mol. Simul.* **2003**, *29*, 677−684.
(2) Arab, M.; Picaud, F.; Devel, M.; Ramseyer, C.; Girardet, C. *Phys. Rev. B: Condens. Mater. Phys.* **2004**, *69*, 165401.
(3) Arora, G.; Sandler, S. I. *J. Chem. Phys.* **2006**, *124*, 084702.
(4) Bienfait, M.; Asmussen, B.; Johnson, M.; Zeppenfeld, P. *Surf. Sci.* **2000**, *460*, 243−248.
(5) Chen, H. B.; Sholl, D. S. *J. Am. Chem. Soc.* **2004**, *126*, 7778−7779.
(6) Duren, T.; Keil, F. J.; Seaton, N. A. *Mol. Phys.* **2002**, *100*, 3741−3751.
(7) Mao, Z.; Sinnott, S. B. *J. Phys. Chem. B* **2001**, *105*, 6916−6924.
(8) Hinds, B. J.; Chopra, N.; Rantell, T.; Andrews, R.; Gavalas, V.; Bachas, L. G. *Science* **2004**, *303*, 62−65.
(9) Skoulidas, A. I.; Sholl, D. S.; Johnson, J. K. *J. Chem. Phys.* **2006**, *124*, 054708−054711.
(10) Sheintuch, M.; Efremenko, I. *Chem. Eng. Sci.* **2004**, *59*, 4739−4746.
(11) Sznejer, G. A.; Efremenko, I.; Sheintuch, M. *AIChE J.* **2004**, *50*, 596−610.
(12) Bhatia, S. K.; Nicholson, D. *AIChE J.* **2006**, *52*, 29−38.
(13) Roy, S.; Raju, R.; Chuang, H. F.; Cruden, B. A.; Meyyappan, M. *J. Appl. Phys.* **2003**, *93*, 4870−4879.
(14) Skoulidas, A. I.; Ackerman, D. M.; Johnson, J. K.; Sholl, D. S. *Phys. Rev. Lett.* **2002**, *89*, 185901-1−185901-4.
(15) Striolo, A. *Nano Lett.* **2006**, *6*, 633−639.
(16) Mao, Z. G.; Sinnott, S. B. *J. Phys. Chem. B* **2000**, *104*, 4618−4624.
(17) Vasenkov, S.; Karger, J. *Phys. Rev. E: Stat. Phys., Plasmas, Fluids, Relat. Interdiscip. Top.* **2002**, *66*, 052601.
(18) Vasenkov, S.; Schuring, A.; Fritzsche, S. *Langmuir* **2006**, *22*, 5728−5733.
(19) Hahn, K.; Karger, J.; Kukla, V. *Phys. Rev. Lett.* **1996**, *76*, 2762−2765.
(20) Meersmann, T.; Logan, J. W.; Simonutti, R.; Caldarelli, S.; Comotti, A.; Sozzani, P.; Kaiser, L. G.; Pines, A. *J. Phys. Chem. A* **2000**, *104*, 11665−11670.
(21) Cheng, C.-Y.; Bowers, C. R. *ChemPhysChem* **2007**. In press.
(22) Kärger, J. *Phys. Rev. A: At., Mol., Opt. Phys.* **1992**, *45*, 4173−4174.
(23) Lutz, C.; Kollmann, M.; Bechinger, C. *Phys. Rev. Lett.* **2004**, *93*, 026001.
(24) Wei, Q. H.; Bechinger, C.; Leiderer, P. *Science* **2000**, *287*, 625−627.
(25) Chou, C. Y.; Eng, B. C.; Robert, M. *J. Chem. Phys.* **2006**, *124*, 044902.
(26) Gorbitz, C. H. *Acta Crystallogr., Sect. B* **2002**, *58*, 849−854.
(27) Moudrakovski, I.; Soldatov, D. V.; Ripmeester, J. A.; Sears, D. N.; Jameson, C. J. *Proc. Natl. Acad. Sci. U.S.A.* **2004**, *101*, 17924−17929.
(28) Soldatov, D. V.; Moudrakovski, I. L.; Grachev, E. V.; Ripmeester, J. A. *J. Am. Chem. Soc.* **2006**, *128*, 6737−6744.
(29) Soldatov, D. V.; Moudrakovski, I. L.; Ripmeester, J. A. *Angew. Chem., Int. Ed.* **2004**, *43*, 6308−6311.
(30) Ueda, T.; Eguchi, T.; Nakamura, N.; Wasylishen, R. E. *J. Phys. Chem. B* **2003**, *107*, 180−185.
(31) Springuelhuet, M. A.; Fraissard, J. *Chem. Phys. Lett.* **1989**, *154*, 299−302.
(32) Ueda, T.; Kurokawa, K.; Eguehit, T.; Kachi-Terajima, C.; Takamizawa, S. *J. Phys. Chem. C* **2007**, *111*, 1524−1534.
(33) Sozzani, P.; Comotti, A.; Simonutti, R.; Meersmann, T.; Logan, J. W.; Pines, A. *Angew. Chem., Int. Ed.* **2000**, *39*, 2695−2698.
(34) Ripmeester, J. A.; Ratcliffe, C. I. *J. Phys. Chem.* **1995**, *99*, 619−622.
(35) Larsen, R. G.; Shore, J.; Schmidtrohr, K.; Emsley, L.; Long, H.; Pines, A.; Janicke, M.; Chmelka, B. F. *Chem. Phys. Lett.* **1993**, *214*, 220−226.

large chemical shift range allows the confined phase to be distinguished from the free gas and reveals interactions with the channel interiors and other Xe atoms in nanotubes.[20,21,27,33,41,42]

Two-dimensional thermally polarized ^{129}Xe exchange NMR spectroscopy (2D-EXSY) has been successfully applied to probe slow exchange among multiple adsorption sites in diverse systems, including liquid crystals,[43,44] zeolites,[35−37] polymers,[40,45,46] and carbon nanotubes.[47,48] To obtain quantitative dynamical information using this method, the mixing-time dependences of the integrated diagonal-peak and cross-peak signals are fit to an appropriate kinetic model. For example, Tallavaara et al. extracted the exchange rates and T_1 times of thermally polarized ^{129}Xe in the liquid-crystal phase confined in controlled-pore glass by fitting the cross- and diagonal-peak mixing-time dependences.[44] Unfortunately, mixing-time dependence studies are usually not feasible in thermally polarized samples due to the acquisition time requirements associated with long relaxation times and low density. While exchange-rate constants and spin-relaxation times can be determined from a 2D-EXSY spectrum acquired at a single mixing time,[36−38,49] thereby minimizing the total experiment time, the accuracy of this method is generally lower than that which can be achieved by acquiring multiple 2D-EXSY spectra at a series of mixing times.[36,44,49,50]

With the advent of continuous flow hyperpolarized (CFHP) ^{129}Xe NMR, it is now possible to overcome conventional sensitivity limitations.[51−54] A flow of hyperpolarized gas through the sample space facilitates rapid acquisition of ^{129}Xe 2D-EXSY spectra because the nuclear spin polarization is replenished on a time scale determined by the gas flow rate through the sample space, not by the typically long ^{129}Xe relaxation times. Moreover, the per-scan sensitivity can be enhanced by 4 orders of magnitude in comparison to the thermally polarized ^{129}Xe spectrum. Although CFHP ^{129}Xe 2D-EXSY is well-suited for studies of gas exchange in nanoporous materials, the information obtained in most of the prior studies employing this method has been of a qualitative nature, such as determination of pore-space geometries, interconnectivities, or exchange pathways.[38−40,54,55] It would appear that extraction of quantitative dynamic information has been hampered by the lack of a kinetic formalism appropriate to the analysis of 2D-EXSY spectra acquired under CFHP conditions. Analytical expressions for the mixing-time dependences of cross-/diagonal-peak signal ratios found in the literature[36,49] are derived by assuming (1) thermally polarized spins in the absence of flow (e.g., in a sealed NMR tube) and (2) equal cross-peak signals for the forward and reverse exchange processes. Nevertheless, the conventional matrix formalism was applied without modification to estimate exchange rates between the gas and pores in a recent CFHP ^{129}X 2D-EXSY study of gas exchange in porous silicon.[38] As the kinetic model presented below reveals, flow effects must be considered when the residence time in the sample space is shorter than the exchange time: $\tau_R < k_{ex}^{-1}$. In this regime, flow attenuates the exchange cross-peaks involving the gas phase, leading to a possible underestimation of the exchange rates. The effects of flow are consistent with the observations reported in ref 55. Moreover, the cross-peaks representing the forward and reverse exchange processes in CFHP ^{129}Xe 2D-EXSY spectra are generally asymmetric with respect to the spectrum diagonal, as discussed in qualitative terms by Anala et al. in a study of the combustion process.[56]

In this article, we demonstrate how CFHP ^{129}Xe 2D-EXSY can be used to detect Xe atoms entering and exiting the channel openings in AV. The mixing-time dependence of the diagonal- and cross-peak signal integrals will be fit to analytical expressions derived by assuming slow exchange between the gas phase and a surface exhibiting Langmuir adsorption. The mean desorption rate is determined under flowing gas conditions at low, moderate, and high fractional steady-state Xe occupancies, yielding semiquantitative information about molecular exchange in the vicinity of the channel openings.

Experimental Section

Polycrystalline AV was purchased from MP Biochemicals and used as received. Scanning electron microscopy of the polycrystalline AV sample revealed rod-shaped crystallites with a distribution of lengths ranging from 20 to 40 μm. A 15-mg sample was packed loosely into a 3.2-mm (inside diameter) cylindrical sample holder machined from PEEK, around which a seven-turn solenoid NMR coil was wound and tuned to the ^{129}Xe resonance frequency of 110.6 MHz. The 90° pulse length was 4 μs. The threaded inlet and outlet of the sample holder were connected to 0.125″ PFA tubing with vacuum-tight fittings. Prior to NMR measurements, the sample space was evacuated to about 10^{-5} mbar at 100 °C for 2−3 h. Spectra were acquired at a field of 9.4 T with a Bruker Avance NMR spectrometer. Rapid accumulation of spectra was achieved by pre-pending the standard 2D-EXSY pulse sequence with a saturating RF pulse train (SAT) followed by a fixed repolarization delay. The modification serves to circumvent the lengthy acquisition recycle delay that would be required using thermally

(36) Moudrakovski, I. L.; Ratcliffe, C. I.; Ripmeester, J. A. *Appl. Magn. Reson.* **1995**, *8*, 385−399.
(37) Moudrakovski, I. L.; Ratcliffe, C. I.; Ripmeester, J. A. *J. Am. Chem. Soc.* **1998**, *120*, 3123−3132.
(38) Knagge, K.; Smith, J. R.; Smith, L. J.; Buriak, J.; Raftery, D. *Solid State Nucl. Magn. Reson.* **2006**, *29*, 85−89.
(39) Moudrakovski, I. L.; Wang, L. Q.; Baumann, T.; Satcher, J. H.; Exarhos, G. J.; Ratcliffe, C. I.; Ripmeester, J. A. *J. Am. Chem. Soc.* **2004**, *126*, 5052−5053.
(40) Simonutti, R.; Bracco, S.; Comotti, A.; Mauri, M.; Sozzani, P. *Chem. Mater.* **2006**, *18*, 4651−4657.
(41) Comotti, A.; Bracco, S.; Ferretti, L.; Mauri, M.; Simonutti, R.; Sozzani, P. *Chem. Commun.* **2007**, 350−352.
(42) Jameson, C. J.; de Dios, A. C. *J. Chem. Phys.* **2002**, *116*, 3805−3821.
(43) Long, H. W.; Luzar, M.; Gaede, H. C.; Larsen, R. G.; Kritzenberger, J.; Pines, A.; Crawford, G. P. *J. Phys. Chem.* **1995**, *99*, 11989−11993.
(44) Tallavaara, P.; Jokisaari, J. *Phys. Chem. Chem. Phys.* **2006**, *8*, 4902−4907.
(45) Schantz, S.; Veeman, W. S. *J. Polym. Sci., Part B: Polym. Phys.* **1997**, *35*, 2681−2688.
(46) Nossov, A.; Guenneau, F.; Springuel-Huet, M. A.; Haddad, E.; Montouillout, V.; Knott, B.; Engelke, F.; Fernandez, C.; Gedeon, A. *Phys. Chem. Chem. Phys.* **2003**, *5*, 4479−4483.
(47) Romanenko, K. V.; Fonseca, A.; Dumonteil, S.; Nagy, J. B.; de Lacaillerie, J. D. B.; Lapina, O. B.; Fraissard, J. *Solid State Nucl. Magn. Reson.* **2005**, *28*, 135−141.
(48) Kneller, J. M.; Soto, R. J.; Surber, S. E.; Colomer, J. F.; Fonseca, A.; Nagy, J. B.; Van Tendeloo, G.; Pietrass, T. *J. Am. Chem. Soc.* **2000**, *122*, 10591−10597.
(49) Perrin, C. L.; Dwyer, T. J. *Chem. Rev.* **1990**, *90*, 935−967.
(50) Ernst, R. R.; Bodenhausen, G.; Wokaun, A. *Principles of Nuclear Magnetic Resonance in One and Two Dimensions*; University Press: Oxford 1987.
(51) Driehuys, B.; Cates, G. D.; Miron, E.; Sauer, K.; Walter, D. K.; Happer, W. *Appl. Phys. Lett.* **1996**, *69*, 1668−1670.
(52) Haake, M.; Pines, A.; Reimer, J. A.; Seydoux, R. *J. Am. Chem. Soc.* **1997**, *119*, 11711−11712.
(53) Zook, A. L.; Adhyaru, B. B.; Bowers, C. R. *J. Magn. Reson.* **2002**, *159*, 175−182.
(54) Seydoux, R.; Pines, A.; Haake, M.; Reimer, J. A. *J. Phys. Chem. B* **1999**, *103*, 4629−4637.
(55) Pawsey, S.; Moudrakovski, I.; Ripmeester, J.; Wang, L. Q.; Exarhos, G. J.; Rowsell, J. L. C.; Yaghi, O. M. *J. Phys. Chem. C* **2007**, *111*, 6060−6067.
(56) Anala, S.; Pavlovskaya, G. E.; Pichumani, P.; Dieken, T. J.; Olsen, M. D.; Meersmann, T. *J. Am. Chem. Soc.* **2003**, *125*, 13298−13302.

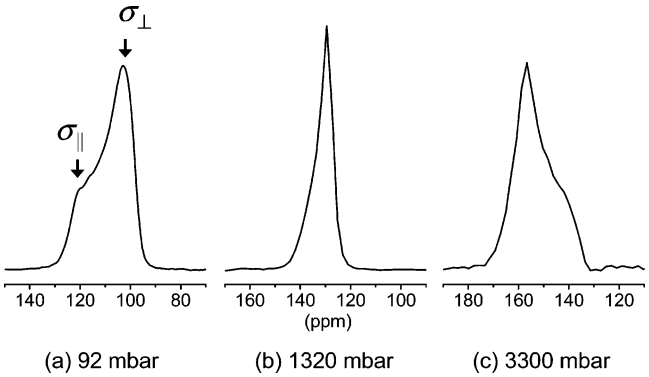

Figure 1. Steady-state continuous flow hyperpolarized ^{129}Xe NMR spectra in AV nanotubes, acquired at −10 °C, at the following Xe partial pressures: (a) 92 mbar, (b) 1320 mbar, (c) 3300 mbar. The chemical shift scale is referenced to dilute Xe gas (0 ppm).

polarized ^{129}Xe NMR due to lengthy T_1 relaxation times and establishes a reproducible polarization distribution as a function of displacement from the channel openings. Prior to each repetition of the 2D-EXSY pulse program, the ^{129}Xe magnetization in the sample space is initially destroyed by the application of a nonselective $\pi/2$ pulse train followed by a repolarization delay of $\tau_1 = 4$ s to allow the build-up of hyperpolarized Xe inside the channels. The complete pulse sequence is

$$(\mathrm{SAT}) - \tau_1 - \pi/2 - t_1 - \pi/2 - \tau_m - \pi/2 - t_2(\mathrm{ACQ})$$

where τ_m is the mixing time. An eight-step phase cycle was employed for coherence transfer pathway selection.[50] It should be noted that under the present experimental conditions only hyperpolarized ^{129}Xe gives rise to observable NMR signals since thermally polarized ^{129}Xe signals cannot be detected without signal averaging. A series of 10 CFHP 2D-EXSY spectra were acquired at −10 °C with mixing times ranging from $\tau_m = 10$ to 600 ms at Xe partial pressures of 92, 1320, and 3300 mbar. Typically, 64 and 1024 points were collected in the t_1 and t_2 dimensions. A line-broadening of 300 Hz was applied in both time dimensions prior to Fourier transformation. Chemical shifts are referenced to dilute Xe gas (0 ppm).

Hyperpolarized ^{129}Xe gas was generated by the home-built continuous flow Rb−Xe spin-exchange optical pumping system described in ref 53. The Xe gas mixture was recirculated through the sample space at a nominal flow rate of 100 mL/min, as measured on a gas flow meter. The experiments at 92 mbar were carried out using a 2%/2%/96% natural isotopic abundance Xe/N_2/He gas mixture (Spectra Gases). At this pressure, the ^{129}Xe spin polarization reached levels as high as about 20%. The total gas pressure was 4600 mbar in all experiments. A mixture of natural abundance ^{129}Xe gas (Praxair) and ^{4}He was used for the experiments at 1320 mbar and 3300 mbar Xe partial pressure. Molar loadings of Xe in AV were estimated from the NMR spectra shown in Figure 1 using the empirical correlation between molar loading and the perpendicular component of the cylindrically symmetric chemical shielding tensor, $\sigma_\perp$, as established from Figure 4 of ref 27: $\theta_m = 0.00536 \cdot \sigma_\perp - 0.51964$ (at 20 °C). Shielding tensor components were extracted from fits to the powder pattern line shapes. Molar loadings were converted to volumetric fractional occupancies (θ) using published adsorption capacity data.[29] Although the experiments presented herein were performed at −10 °C, the temperature dependence of $\sigma_\perp$ (at constant θ_m) is assumed to be only weak since $\sigma_\perp$ depends primarily on Xe−Xe interactions.[41,42]

Results and Discussion

Xenon adsorption in self-assembled AV nanotubes is known to obey the Langmuir equation[29] where the steady-state fractional occupancy is given by θ = occupied sites/total sites = $Kp/(1 + Kp)$, $K = k_a/k_d$ is the equilibrium constant, and p is the Xe partial pressure. By varying p at constant T, the effect of occupancy on the exchange rate can be explored under steady-state adsorption conditions. Figure 1 presents the one-dimensional CFHP ^{129}Xe spectra in AV at Xe partial pressures of 92, 1320, and 3300 mbar at −10 °C. The chemical shielding anisotropy exhibits a sign inversion at $\theta \approx 0.4$ due to the relative contributions of Xe−Xe and Xe−wall interactions to the perpendicular and parallel components of the shielding tensor,

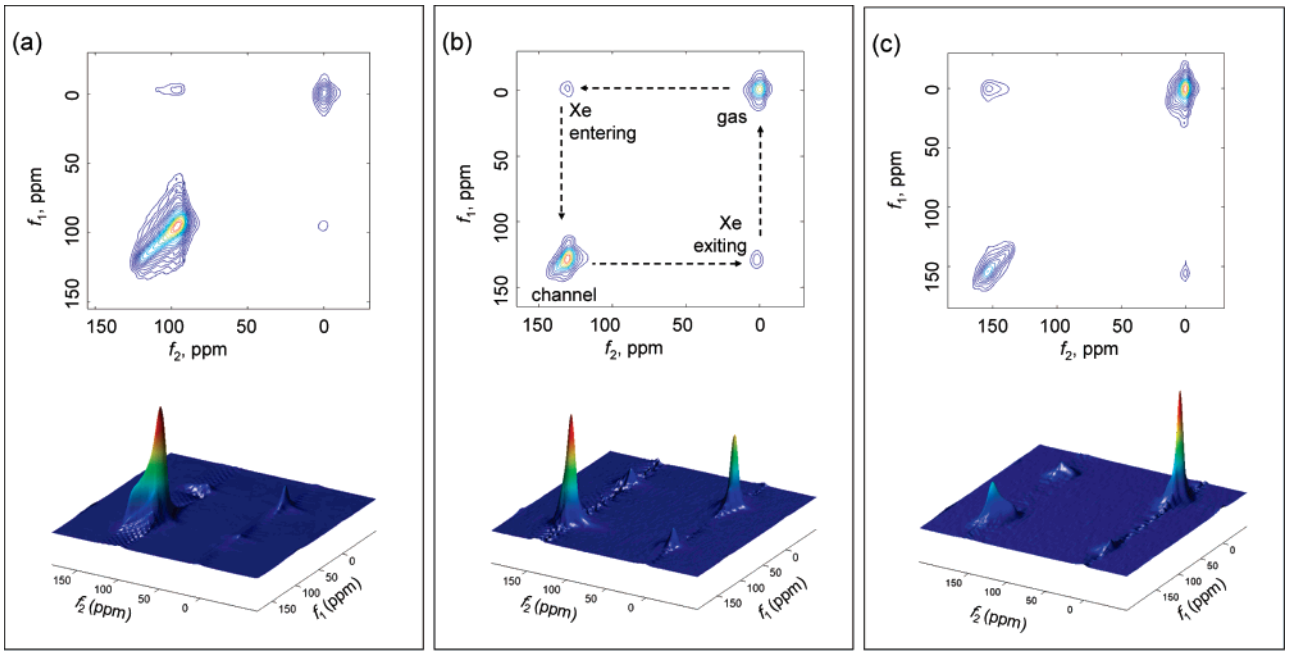

Figure 2. Continuous flow hyperpolarized ^{129}Xe 2D-EXSY spectra in AV nanotubes at −10 °C acquired at the mixing times yielding maximum cross-peak intensities: (a) 92 mbar, $\tau_m = 35$ ms; (b) 1320 mbar, $\tau_m = 100$ ms; (c) 3300 mbar, $\tau_m = 100$ ms. The spectra were recorded with 64 × 1024 data points with 8 scans per spectrum. A Gaussian line-broadening of 300 Hz was applied in both time dimensions. The total experiment time per 2D spectrum with $\tau_1 = 4$ s was about 30 min.

Table 1. Best-Fit Kinetic Parameters for CFHP ^{129}Xe 2D-EXSY Spectra in AV at −10 °C; Uncertainties Represent 95% Confidence Intervals

			channel → channel	gas → gas	gas → channel eq 7		channel → gas eq 8	
p_{Xe}/mbar	θ	K/bar^{-1}	$\bar{k}_d^{diag}$/s^{-1}	τ_R/ms	$\bar{k}_d$/s^{-1}	τ_R/ms	$\bar{k}_d$/s^{-1}	τ_R/ms
92	0.047	0.52 ± 0.03	2.5 ± 1	19 ± 3	6.1 ± 2	19 (fixed)	3.2 ± 1	19 (fixed)
					4.2 ± 2	11 ± 5	2.2 ± 1.4	13.4 ± 5
1320	0.39	0.48 ± 0.15	1.5 ± 0.6	68 ± 35	–	68 (fixed)	–	68 (fixed)
					2.3 ± 0.5	35 ± 3	2.7 ± 0.5	43 ± 3
3300	0.64	0.54 ± 0.08	n/a	28 ± 5	1.9 ± 0.8	28 (fixed)	<2.2	28 (fixed)
					–	–	–	–

respectively.[27,33,41,42] At 92 mbar, the anisotropy is dominated by the Xe−wall interactions (Figure 1a), while at 3300 mbar (Figure 1c), Xe−Xe interactions dominate. Validating the assumption of Langmuir adsorption, the estimated equilibrium constants reported in Table 1 are within experimental error the same at all three pressures.

The ^{129}Xe 2D-EXSY spectra at 92, 1320, and 3300 mbar are presented in Figure 2. The gas → channel and channel → gas cross-peaks are strongly attenuated by the gas flow rate which limits the residence time τ_R of gas atoms in the sample space. The observation of gas atoms entering (upper left cross-peak) and exiting (lower right cross-peak) the single-file nanotubes is evidenced by the appearance of cross-peaks. Elongated diagonal-peaks due to Xe which did not exchange during τ_m are observed at 92 mbar (Figure 2a) and 3300 mbar (Figure 2c), while the contours of the diagonal-peak at 1320 mbar exhibit a roughly circular shape (Figure 2b). As in the 1D spectra presented in Figure 1, the shape of the adsorbed-phase diagonal-peaks in the 2D-EXSY spectra reflects the distribution of AV crystallites with different orientations with respect to the magnetic field. Cross-peaks corresponding to Xe exchange between different individual channel orientations are not observed, indicating that multiple Xe exchange events between different channels cannot be detected under these experimental conditions.

To obtain analytical expressions for the mixing-time dependence of the diagonal- and cross-peak signals, we start with the following rate equations for the gas- and adsorbed-phase magnetizations, M_g and M_c, assuming steady-state adsorption on a Langmuir surface:

$$\frac{dM_g}{dt} = -k_d\frac{n_c\theta}{n_g}M_g + k_dM_c - \frac{M_g}{T_{1g}} + \frac{M_i - M_g}{\tau_R} \quad (1)$$

$$\frac{dM_c}{dt} = k_d\frac{n_c\theta}{n_g}M_g - k_dM_c - \frac{M_c}{T_{1c}} \quad (2)$$

where $n_c/n_g \equiv$ ratio of total adsorption sites to gas atoms, $k_d \equiv$ desorption rate constant, and M_i is the magnetization in one sample holder void space volume of freshly hyperpolarized gas. The longitudinal nuclear spin-relaxation times of Xe inside the channels and in the gas phase are given by T_{1c} and T_{1g}. For Xe in AV at 9.4 T, $T_{1c} = 50 - 150$ s, depending on θ,[21] and $T_{1g} > 600$ s. Since the repolarization delay of $\tau_1 = 4$ s during which the hyperpolarized atoms enter and diffuse into the channels is much shorter than either spin-relaxation time, the spin-relaxation terms can be neglected. Assuming an excess of Xe gas (i.e., $n_c\theta/n_g \ll 1$), the repolarization of the gas during τ_1 will be dominated by the influx of freshly hyperpolarized gas into the sample space gas. This assumption is validated by the observation that selective saturation of the nanotube phase ^{129}Xe transition did not significantly affect the gas-phase signal.[21] The initial magnetizations in the gas and channels at the beginning of the mixing delay are as follows:

$$M_g^\circ \equiv M_g(\tau_1) \approx M_i(1 - e^{-\tau_1/\tau_R}) \quad (3)$$

$$M_c^\circ \equiv M_c(\tau_1) \approx M_i\left[\frac{n_c\theta}{n_g}\right]\frac{(1 - e^{-k_d\tau_1})\tau_R^{-1} - (1 - e^{-k_d\tau_1})k_d}{\tau_R^{-1} - k_d} \quad (4)$$

Longitudinal magnetizations that do not exchange during τ_m yield the "diagonal" peaks in the 2D-EXSY spectrum. The gas-phase and channel diagonal-peaks are expected to decay monoexponentially:

$$M_{g\to g}(\tau_1,\tau_m) = M_g^o \exp\left[-\tau_m\left(\frac{1}{\tau_R} + k_d\frac{n_c\theta}{n_g}\right)\right] \quad (5)$$

$$M_{c\to c}(\tau_1,\tau_m) = M_c^o\, e^{-k_d\tau_m} \quad (6)$$

The mixing time dependence of the longitudinal magnetizations representing Xe entering and exiting the channels during the mixing time (assuming excess gas) are as follows:

$$M_{g\to c}(\tau_1,\tau_m) = M_g^o\frac{k_d}{\tau_R^{-1} - k_d}\frac{n_c\theta}{n_g}(e^{-k_d\tau_m} - e^{-\tau_m/\tau_R}) \quad (7)$$

$$M_{c\to g}(\tau_1,\tau_m) \approx M_c^o\frac{k_d}{\tau_R^{-1} - k_d}(e^{-k_d\tau_m} - e^{-\tau_m/\tau_R}) \quad (8)$$

The expressions reveal that the cross-peaks will generally have unequal amplitudes, vanish in the limit $\tau_R \to 0$ or $k_d \to 0$, and are significantly affected by the flow when $\tau_R^{-1} > k_d$. The time dependence of the two cross-peaks will be the same in this model, and each is predicted to pass through a maximum at

$$\tau_m^{max} = \frac{\ln(k_d\tau_R)}{(k_d - \tau_R^{-1})}$$

Equations 7 and 8 pertain to a homogeneous surface consisting of n_c adsorption sites. Though Xe in AV exhibits a Langmuir adsorption isotherm, it is important to note that the average channel length in our AV sample is roughly 5 orders of magnitude greater than the diameter of a Xe. For an atom to escape from within the channel, it must first diffuse to the opening where it must then overcome a potential energy barrier. In ref 21 we postulated that the diffusion-limited exchange kinetics in one-dimensional pores can be modeled by taking a distribution of desorption rates:

$$k_d \approx \tau_d^{-1} = \frac{(F/\pi)^2}{\bar{z}^4}$$

for single-file diffusion, where F is the single-file mobility, $\bar{z}$ is the mean displacement from the channel opening, and τ_d is the diffusion time or

$$k_d \approx \tau_d^{-1} = \frac{(D_0/\pi)}{\bar{z}^2}$$

for normal one-dimensional diffusion. In the present work, the distribution $k_d(z)$ will be replaced by a single mean value, $\bar{k}_d$. This simplified treatment should yield semiquantitative results at sufficiently short mixing times.

Figure 3 presents the τ_m dependence of the cross- and diagonal-peak integrals along with the nonlinear least-squares fits to eq 5−8. The fitted values for $\bar{k}_d$ and τ_R at each pressure are reported in Table 1. Although a monoexponential decay of the gas-phase diagonal-peak is expected from eq 5, a biexponential function yielded better fits. However, the pre-exponential factors obtained from least-squares fitting show that the more rapidly decaying exponential term of the two accounts for about 90% of the initial gas-phase diagonal-peak signals at 92 and 3300 mbar. Although the 2D-EXSY spectra were acquired at a nominal flow rate of 100 mL/min at all three pressures (as indicated by the flow meter), no correction was made for gas composition. The actual residence times at 1320 mbar and 3300 mbar appear to have been substantially longer than in the experiments at 92 mbar. The gas-phase diagonal-peak at 1320 mbar yielded $\tau_R = 68$ ms.

To assess the validity of the kinetic model, fits to each of the cross-peak mixing time dependences at each pressure were performed in two different ways: by either fixing τ_R to the value established from the gas-phase diagonal-peak in the same spectrum, or by allowing all three parameters ($\bar{k}_d$,τ_R, and the pre-exponential factor) to vary freely. The parameters resulting from the two and three parameter least-squares fits are reported in Table 1 as the upper- and lower-row entries for $\bar{k}_d$ and τ_R at each of the three pressures studied. Where no table entries are reported, the fits did not exhibit good qualitative agreement with the experimental data.

Despite the large relative errors, the cross-peak fits reveal a clear decrease in the rate constant $\bar{k}_d$ upon increasing the occupancy from $\theta = 0.047$ (92 mbar) to 0.39 (1320 mbar). The trend is more pronounced for the gas (g) → channel (c) process. At 92 mbar (low occupancy), reasonable self-consistency of the model (eqs 1−8) was obtained. The residence time extracted from the decay of $M_{g\rightarrow g}$ is within the 95% confidence interval of the values obtained from the fits to both cross-peaks. However, the best-fit desorption rate for the g → c (Xe entering) process was about a factor of 2 higher than that for the c → g (Xe exiting) process. This asymmetry might be attributed to one or more of the following factors which are not accounted for by our simplified model: presence of a desorption barrier, channel boundary effects, or one-dimensional diffusion effects.

At 3300 mbar, where the occupancy is relatively high, the fixed value for the residence time of 28 ms (obtained from the diagonal-peak decay) yielded good qualitative fits to the cross-peaks, and close agreement between the $\bar{k}_d$ values obtained from the c → g and g → c cross-peaks was obtained. Allowing τ_R to vary yielded poor agreement to the data at this pressure due to low signal-to-noise of the cross-peaks. At 1320 mbar, holding $\tau_R = 68$ ms constant yielded unacceptable two-parameter fits of the cross-peaks (not shown). We do not have an explanation for this irregularity. Nevertheless, the three-parameter cross-peak fits allowing τ_R to vary freely gave self-consistent results, and $\bar{k}_d$ obtained from the entering and exiting processes, are in agreement.

Several factors could account for the observed decrease in $\bar{k}_d$. A decrease in the rate with occupancy might be explained by the observed −7.4 kJ/mol increase in the enthalpy of desorption upon increasing the pressure from 92 mbar to 1320 mbar at −10 °C,[57] a change which would be expected to reduce k_d by a factor of about 10^2. However, the actual reduction is only by a factor of about 3, implying diffusion-limited rather than thermodynamic-limited desorption. For SFD, which has been confirmed in AV for time scales longer than about 0.5 s, the mean squared displacement increases according to $\langle z^2 \rangle = 2F\sqrt{t}$, where F is the single-file mobility. For hard-sphere particles in cylindrical channels, $F \propto (1 - \theta)/\theta$.[22] Thus, the observed reduction in desorption rate upon increasing the occupancy is consistent with a decrease in the diffusivity in the channels.

As shown in Figure 3d, the diagonal-peak representing Xe which remains in the channels throughout the exchange delay also exhibited a decrease in $\bar{k}_d^{diag}$ with increasing occupancy, but the rates are slightly lower than those extracted from the cross-peaks. This result can be explained qualitatively in terms of diffusion-limited gas exchange. The cross-peak signals arise from atoms close enough to the channel openings to escape during the finite residence time. In contrast, the diagonal-peak includes signal contributions from all Xe atoms which have diffused into the channels during the longer repolarization delay of $\tau_1 = 4$ s. For this larger ensemble of Xe atoms, the mean diffusion time to return to the channel opening is longer, consistent with an apparent reduction in the desorption rate.

While the single-file mobility of Xe in AV nanotubes is unknown, a rough estimate of the mean displacement can be made from previously measured single-file mobilities in zeolites with 1D channels. For example, a PFG NMR study[19] of CF_4 (4.7 Å) in $AlPO_4$-5 zeolite (8.2 Å cylindrical channels) at moderate occupancy yielded $F \approx 1 \times 10^{-12}$ m^2 s$^{-1/2}$, while a quasi-elastic neutron diffraction study[58] of CH_4 (3.8 Å) in zeolite-48 (5.3 × 5.6 Å) yielded $F = 2 \times 10^{-12}$ m^2 s$^{-1/2}$. Assuming a similar single-file mobility for Xe in AV, the atoms would reach a depth of ∼2 μm during the repolarization delay, with $\tau_1 = 4$ s. The residence time of Xe atoms in the sample space limits the cross-peak intensities. At the flow rate used in the present study, the maximum cross-peak intensities were observed at ∼50 ms, where the exchange is limited to polarized atoms within ∼0.7 μm of the channel opening. Interrupting the gas flow momentarily during the exchange delay is envisaged as a means to increase cross-peak intensities. By increasing the residence time, it should be possible to probe the kinetics of desorption over a much wider range of length scales or intercrystalline exchange between nanotubes with different orientations.

(57) Cheng, C.-Y.; Bowers, C. R. Unpublished results.
(58) Jobic, H.; Hahn, K.; Karger, J.; Bee, M.; Tuel, A.; Noack, M.; Girnus, I.; Kearley, G. *J. Phys. Chem. B* **1997**, *101*, 5834−5841.

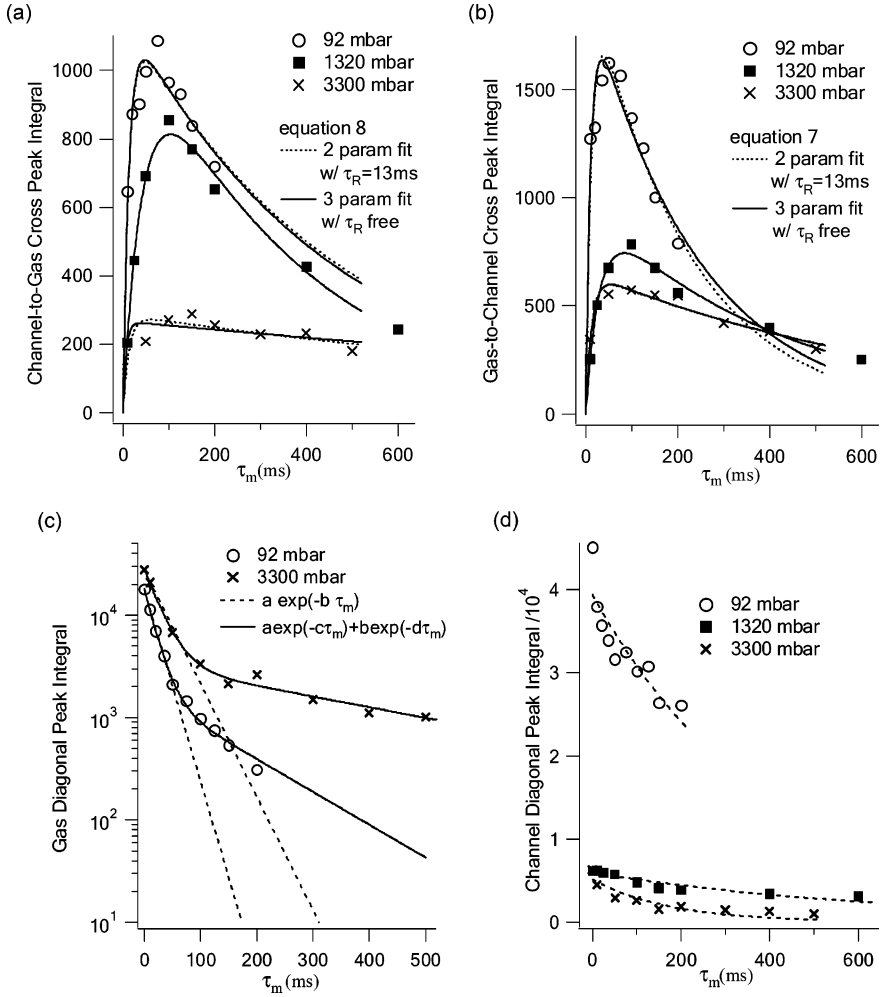

Figure 3. Mixing-time dependences of cross- and diagonal-peak signal integrals in CFHP ^{129}Xe 2D-EXSY spectra of AV nanotubes at −10 °C. (a) Channel-to-gas cross-peak signal integrals and least-squares fits at three Xe pressures. (b) Gas-to-channel cross-peak integrals. (c) Gas-to-gas diagonal-peak mixing-time dependences. The solid and dashed curves represent the fits to the functions given in the legend. (d) Channel-to-channel diagonal-peak mixing-time dependences. The dashed lines represents the least-squares fits to a single-exponential decay function.

Conclusions

Direct observation of atoms entering and exiting self-assembled L-alanyl-L-valine nanotubes has been facilitated by continuous flow hyperpolarized ^{129}Xe two-dimensional exchange NMR spectroscopy. Analytical solutions for the mixing-time dependence of the diagonal- and cross-peak signals have been obtained under flow conditions with excess Xe gas, revealing that the effects of flow need to be considered when $\tau_R^{-1} > k_d$, as is the case for Xe in AV under our experimental conditions. Nonlinear least-squares fitting to these expressions yielded the effective rate of Xe escape from the AV channels. Although the assumption of a single mean desorption rate (as opposed to a distribution of rates) probably contributes to the relatively large uncertainties in the fitted values of the desorption rate constants, a reduction in the effective rate of desorption with increasing Xe density has been clearly observed. This finding is consistent with a decrease in the Xe mobility of the channels in the diffusion-limited exchange regime. While single-file diffusion of Xe in AV has been confirmed at longer time scales,[21] the semiquantitative analysis of the present work precludes any definite conclusions to be made concerning the relative importance of normal one-dimensional diffusion versus single-file diffusion to the exchange process. Nonetheless, our study has shown how hyperpolarized xenon-129 NMR can be applied to the investigation of gas-exchange dynamics in nanotubes, and the kinetic model developed herein should serve as a starting point for future hyperpolarized NMR studies of adsorption, diffusion, and exchange processes in nanotubes and other nanoporous materials.

Acknowledgment. We gratefully acknowledge helpful discussions with Cynthia J. Jameson (University of Illinois at Chicago, Department of Chemistry) and Sergey Vasenkov (University of Florida, Department of Chemical Engineering). Construction of the Xenon-129 polarizer was supported by the NHMFL In-House Research Program and the University of Florida.

JA074563N